RESEARCH MEMORANDUM

WIND-TUNNEL INVESTIGATION OF EFFECTS OF VENTRAL FINS AT TWO POSITIONS ON LATERAL-STABILITY DERIVATIVES OF 45° SWEPT HIGH-WING MODEL OSCILLATING IN YAW

By Byron M. Jaquet

Langley Aeronautical Laboratory
Langley Field, Va.

CLASSIFIED DOCUMENT

NATIONAL ADVISORY COMMITTEE
FOR AERONAUTICS

WASHINGTON

December 26, 1956

NACA RM L56J31a

[redacted]

NATIONAL ADVISORY COMMITTEE FOR AERONAUTICS

RESEARCH MEMORANDUM

WIND-TUNNEL INVESTIGATION OF EFFECTS OF VENTRAL FINS AT TWO POSITIONS ON LATERAL-STABILITY DERIVATIVES OF 45° SWEPT HIGH-WING MODEL OSCILLATING IN YAW

By Byron M. Jaquet

SUMMARY

An investigation was made in the Langley stability tunnel to determine the effects of ventral fins at two positions (0° and -70° dihedral) on the lateral stability derivatives of a 45° swept high-wing model oscillating in yaw. The effect of the ventral fins on the stability derivatives was determined with and without the vertical and horizontal tails for an angle-of-attack range of 0° to 30° at a Mach number of 0.13 and a Reynolds number of 0.83×10^6, based on the wing mean aerodynamic chord. The steady-state derivatives for a similar model without ventral fins are also presented. No discussion of the data has been made in order to expedite their publication.

INTRODUCTION

Maintaining sufficient directional stability at supersonic flight conditions has become a difficult problem for designers of airplanes. In many cases, the vertical tail, being in a position where it is greatly influenced by the wing and fuselage wakes, loses its effectiveness at comparatively low angles of attack. (See refs. 1 and 2, for example.) The advantage of using a ventral fin to provide additional directional stability is indicated in reference 3. Two serious disadvantages of the fixed ventral fin are that the landing angle is restricted and the aspect ratio of the ventral fin must be low in order to prevent further landing-angle restrictions. To overcome these deficiencies, one aircraft manufacturer has suggested the use of twin ventral fins which would be used at 0° dihedral for landing and take-off and at -70° dihedral for other flight conditions.

The purpose of the present investigation was to determine the effects at low speed of ventral fins at two positions (dihedral 0° and -70°) on

[redacted]

the lateral stability derivatives of a 45° swept high-wing model oscillating in yaw. The steady-state static lateral stability derivatives of similar models (without ventral fins) are presented in reference 4.

SYMBOLS

The data presented herein are referred to the stability system of axes (fig. 1) which have their origin at the projection of the quarter-mean-aerodynamic-chord point of the wing on the fuselage reference line. The coefficients and symbols are defined as follows:

C_l	rolling-moment coefficient, $\frac{\text{Rolling moment}}{qS_w b_w}$
C_n	yawing-moment coefficient, $\frac{\text{Yawing moment}}{qS_w b_w}$
b	span, ft
S	total area, sq ft
S_e	exposed area, sq ft
l	tail length, distance parallel to fuselage center line from $\bar{c}_w/4$ to $\bar{c}/4$ of tail, ft
c	local chord parallel to plane of symmetry, ft
$\bar{c}$	mean aerodynamic chord, $\frac{2}{S}\int_0^{b/2} c^2 dy$, ft
q	dynamic pressure, lb/sq ft, $\frac{\rho V^2}{2}$
ρ	mass density of air, slugs/cu ft
V	free-stream velocity, ft/sec
α	angle of attack, deg
β	angle of sideslip, radians
$\dot{\beta}$	rate of change of angle of sideslip with time, radians/sec

[redacted]

ψ angle of yaw, radians

$\dot{\psi}$ rate of change of angle of yaw with time, radians/sec

r yawing angular velocity, $\dot{\psi}$, radians/sec

$\dot{r}$ yawing angular acceleration, $\ddot{\psi}$, radians/sec

k reduced-frequency parameter, $\frac{\omega b_w}{2V}$

ω circular frequency of oscillation, $2\pi f$, radians/sec

f frequency of oscillation, cycles/sec

y spanwise distance measured from and perpendicular to plane of symmetry, ft

$$C_{l_\beta} = \frac{\partial C_l}{\partial \beta}$$

$$C_{n_\beta} = \frac{\partial C_n}{\partial \beta}$$

$$C_{l_r} = \frac{\partial C_l}{\partial \frac{rb}{2V}}$$

$$C_{n_r} = \frac{\partial C_n}{\partial \frac{rb}{2V}}$$

$$C_{l_{\dot{\beta}}} = \frac{\partial C_l}{\partial \frac{\dot{\beta} b}{2V}}$$

$$C_{n_{\dot{\beta}}} = \frac{\partial C_n}{\partial \frac{\dot{\beta} b}{2V}}$$

$$C_{l_{\dot{r}}} = \frac{\partial C_l}{\partial \frac{\dot{r} b^2}{4V^2}}$$

[redacted]

$$C_{n_{\dot{r}}} = \frac{\partial C_n}{\partial \frac{\dot{r}b^2}{4V^2}}$$

Subscripts:

f	ventral fin
h	horizontal tail
v	vertical tail
w	wing
ω	parameter measured under oscillatory conditions

MODEL AND APPARATUS

Model

The model used in the present investigation is shown in figure 2. The fuselage was constructed of balsa with fiber-glass covering. The wing and tail assembly (vertical and horizontal) were constructed of a balsa core about which was moulded a plastic material. The wing had spruce spars to assure rigidity. The ventral fins, constructed of $\frac{7}{32}$ inch balsa, had beveled trailing edges and rounded leading edges. A canopy was on the model at all times. Additional details of the model are given in tables I to III.

Tunnel and Oscillation Equipment

The tests were made in the 6- by 6-foot test section of the Langley stability tunnel (ref. 5) with the walls at zero curvature.

The equipment used to oscillate the model is shown in figure 3 and is basically that used in the investigation of reference 6 except that V-belts and pulleys were used for the present investigation in place of the gear reduction unit. The connecting rod was pinned to an eccentric on the flywheel and transmitted a sinusoidal yawing motion to the model.

[redacted]

Recording Equipment

The recording of data was accomplished by the equipment described in detail in reference 7. A part of this equipment was a sine-cosine resolver which was attached, through a thin shaft, to the flywheel and modified the output signals from resistance-type strain gages used to measure the rolling and yawing moments so that the measured signals were proportional to the in-phase and out-of-phase components of the gage signals. These signals were read visually on a highly damped direct-current meter; and the readings, when multiplied by the appropriate constants, gave the aerodynamic derivatives:

$$C_{l_{\beta,\omega}} + k^2 C_{l_{\dot{r},\omega}}$$

$$C_{n_{\beta,\omega}} + k^2 C_{n_{\dot{r},\omega}}$$

$$C_{l_{r,\omega}} - C_{l_{\dot{\beta},\omega}}$$

$$C_{n_{r,\omega}} - C_{n_{\dot{\beta},\omega}}$$

In order to eliminate inertia effects, the wind-off values of these derivatives were subtracted from their respective wind-on values.

TESTS AND CORRECTIONS

The model was tested through an angle-of-attack range of 0° to 30° at 5° increments with the exception of one case where, in order to avoid a resonant condition, an angle of attack of 26° was tested instead of 25°. The amplitude of yaw was $\pm 4^\circ$ and the frequency of oscillation was $1\frac{1}{2}$ cycles per second. The reduced-frequency parameter k was equal to 0.0843. The Mach number was 0.13, the Reynolds number (based on the wing mean aerodynamic chord) was 0.83×10^6, and the dynamic pressure was 24.9 pounds per square foot. With the complete model and with the tail assembly off (vertical and horizontal) the ventral fins were tested at 0° and -70° dihedral for the previously stated test conditions. The tests were also made with the ventral fins off.

[redacted]

It should be noted that the ventral fins were behind the strut for all tests. The wing-fuselage combination with the ventral fins at -70° was inverted and tested at angles of attack of 0°, 10°, and 20° to determine the influence of the strut.

The data are uncorrected for support-strut tares, blocking, or jet-boundary effects.

RESULTS

The effect of the ventral fins on the in-phase derivatives $C_{n_{\beta,\omega}} + k^2 C_{n_{\dot{r},\omega}}$ and $C_{l_{\beta,\omega}} + k^2 C_{l_{\dot{r},\omega}}$ and the out-of-phase derivatives $C_{n_{r,\omega}} - C_{n_{\dot{\beta},\omega}}$ and $C_{l_{r,\omega}} - C_{l_{\dot{\beta},\omega}}$ for the model with the tail assembly off and on are presented in figures 4 and 5, respectively. The increments in these derivatives caused by the ventral fins are shown in figure 6. Also presented in figures 4 and 5 are steady-state derivatives previously obtained in the Langley stability tunnel for a similar model without ventral fins. This model was model D of reference 1, except for the difference in size.

As mentioned previously in the section entitled "Tests," the wing-fuselage combination with the ventral fins at -70° dihedral was tested in an inverted position (to remove the fins from behind the strut) at angles of attack of 0°, 10°, and 20°. These data are not presented herein, but it should be noted that when tested in this manner the damping in yaw was almost identical to that presented in figure 5. The directional stability was slightly more favorable (by about 0.03 at each angle) than the corresponding curve in figure 4; the values of $C_{l_{\beta,\omega}} + k^2 C_{l_{\dot{r},\omega}}$ and $C_{l_{r,\omega}} - C_{l_{\dot{\beta},\omega}}$ tended to be more positive, probably because of a change in wing loading due to the strut projecting from the upper surface of the wing.

CONCLUDING REMARKS

An investigation was made in the Langley stability tunnel to determine the effects of ventral fins at two positions on the lateral stability

derivatives of a 45° swept high-wing model oscillating in yaw. The data are presented without discussion in order to expedite publication.

Langley Aeronautical Laboratory,
National Advisory Committee for Aeronautics,
Langley Field, Va., October 16, 1956.

[redacted]

REFERENCES

1. Smith, Willard G., and Ball, Louis H.: Static Lateral-Directional Stability Characteristics of Five Contemporary Airplane Models From Wind-Tunnel Tests at High Subsonic and Supersonic Speeds. NACA RM A55J03, 1956.

2. Edwards, S. Sherman: Some Interference Effects That Influence Vertical-Tail Loads at Supersonic Speeds. NACA RM A55H30, 1956.

3. Spearman, M. Leroy, and Henderson, Arthur, Jr.: Some Effects of Aircraft Configuration on Static Longitudinal and Directional Stability Characteristics at Supersonic Mach Numbers Below 3. NACA RM L55L15a, 1956.

4. Letko, William: Experimental Investigation at Low Speed of the Effects of Wing Position on the Static Stability of Models Having Fuselages of Various Cross Section and Unswept and 45° Sweptback Surfaces. NACA TN 3857, 1956.

5. Bird, John D., Jaquet, Byron M., and Cowan, John W.: Effect of Fuselage and Tail Surfaces on Low-Speed Yawing Characteristics of a Swept-Wing Model As Determined in Curved-Flow Test Section of the Langley Stability Tunnel. NACA TN 2483, 1951. (Supersedes NACA RM L8G13.)

6. Fisher, Lewis R.: Experimental Determination of the Effects of Frequency and Amplitude on the Lateral Stability Derivatives for a Delta, a Swept, and an Unswept Wing Oscillating in Yaw. NACA RM L56A19, 1956.

7. Queijo, M. J., Fletcher, Herman S., Marple, C. G., and Hughes, F. M.: Preliminary Measurements of the Aerodynamic Yawing Derivatives of a Triangular, a Swept, and an Unswept Wing Performing Pure Yawing Oscillations, With a Description of the Instrumentation Employed. NACA RM L55L14, 1956.

[redacted]

TABLE I.- PERTINENT DETAILS OF MODELS

Fuselage:	
Length, in.	50
Ratio of nose length to rearward length	1.563
Maximum height and width, in.	5.40
Fineness ratio	9.26
Side area, sq in.	212.7
Volume, cu in.	964.4
Maximum cross-sectional area, sq in.	28.3
Vertical tail:	
Total area to fuselage center line, S_v, sq in.	68.7
Exposed area, $S_{e,v}$, sq in.	54.5
Span from fuselage center line, in.	9.81
Root chord, in.	8.76
Mean aerodynamic chord, in.	7.17
Sweepback of quarter-chord line, deg	45
Taper ratio	0.6
Aspect ratio	1.4
NACA airfoil section parallel to root chord	65A008
Tail volume, $\frac{l_v S_v}{b_w S_w}$	0.1136
Canopy:	
Length, in.	14.00
Side area, sq in.	11.9
Maximum cross-sectional area, sq in.	2.0
Volume, cu in.	15.1
Ratio of length to maximum width	5.99
Ratio of distance from fuselage nose to fuselage width	1.11
Wing:	
Area, sq in.	324.0
Span, in.	31.18
Root chord, in.	12.99
Mean aerodynamic chord, in.	10.63
Sweepback of quarter-chord line, deg	45
Taper ratio	0.6
Aspect ratio	3
NACA airfoil section parallel to the plane of symmetry	65A008
Horizontal tail:	
Total area, sq in.	64.8
Span, in.	16.10
Root chord, in.	5.03
Mean aerodynamic chord, in.	4.11
Sweepback of quarter-chord line, deg	45
Taper ratio	0.6
Aspect ratio	4
NACA airfoil section parallel to plane of symmetry	65A008
Tail volume, $\frac{l_h S_h}{\bar{c}_w S_w}$	0.324
Ventral fin (dimensions of one panel unless otherwise noted):	
Total area to hinge line, sq in.	16.3
Span from hinge line to tip, in.	4.58
Root chord on hinge line, in.	5.32
Mean aerodynamic chord, in.	3.86
Sweepback of quarter-chord line, deg	45
Taper ratio	0.34
Aspect ratio	1.29
Airfoil section	Modified flat plate
Distance from $\bar{c}_w/4$ to leading edge of root chord on hinge line, in.	6.82
Distance between hinge lines of right and left panels, fraction of one panel span	0.698
Distance from leading edge of root to $\bar{c}_f/4$, in.	3.21
Ratio of total area of both panels to exposed vertical-tail area	0.60

[redacted]

TABLE II.- FUSELAGE COORDINATES

[Fineness ratio 8.34]

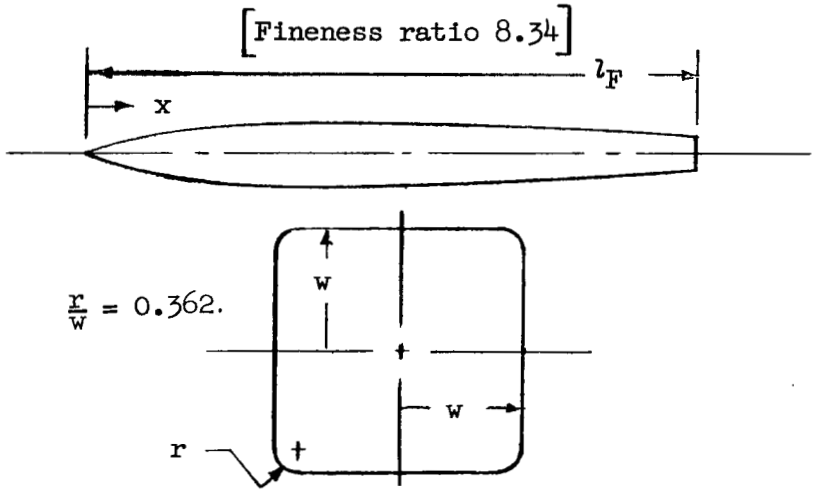

x/l_F	w/l_F
0	0
.04	.012
.08	.022
.12	.030
.16	.038
.20	.043
.24	.048
.28	.051
.32	.053
.36	.054
.40	.054
.44	.054
.48	.054
.52	.054
.56	.053
.60	.052
.64	.051
.68	.049
.72	.048
.76	.046
.80	.043
.84	.040
.88	.038
.92	.034
.96	.031
1.00	.027

TABLE III.- CANOPY COORDINATES

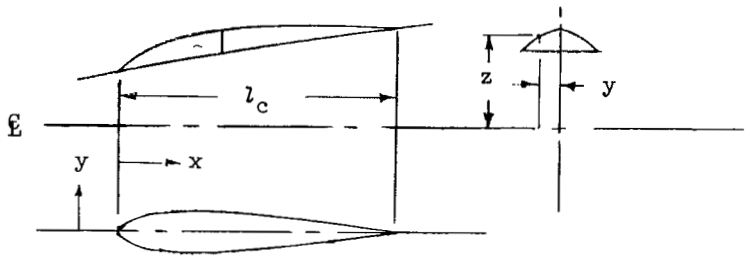

l_c = 14.00 inches

x/l_c	y/l_c	z/l_c
0	0	0.108
.018	.025	.111
	0	.122
.036	.032	.114
	0	.136
.071	.046	.121
	.039	.132
	.031	.143
	.021	.154
	0	.164
.143	.063	.134
	0	.211
.214	.073	.145
	.066	.161
	.059	.179
	.049	.196
	.038	.214
	.024	.232
	0	.241
.286	.079	.155
	0	.259
.357	.082	.164
	0	.269

x/l_c	y/l_c	z/l_c
0.429	0.084	0.171
	.080	.179
	.071	.196
	.061	.214
	.051	.232
	.036	.250
	.014	.268
	0	.271
.500	.081	.179
	0	.268
.571	.073	.183
	0	.261
.643	.063	.186
	.057	.196
	.046	.214
	.032	.232
	.009	.250
	0	.252
.714	.052	.190
	0	.241
.786	.039	.191
	0	.229
.857	.026	.193
	.019	.200
	.016	.207
	.006	.214
	0	.216
.928	.013	.193
	0	.204
1.000	0	.193

[redacted]

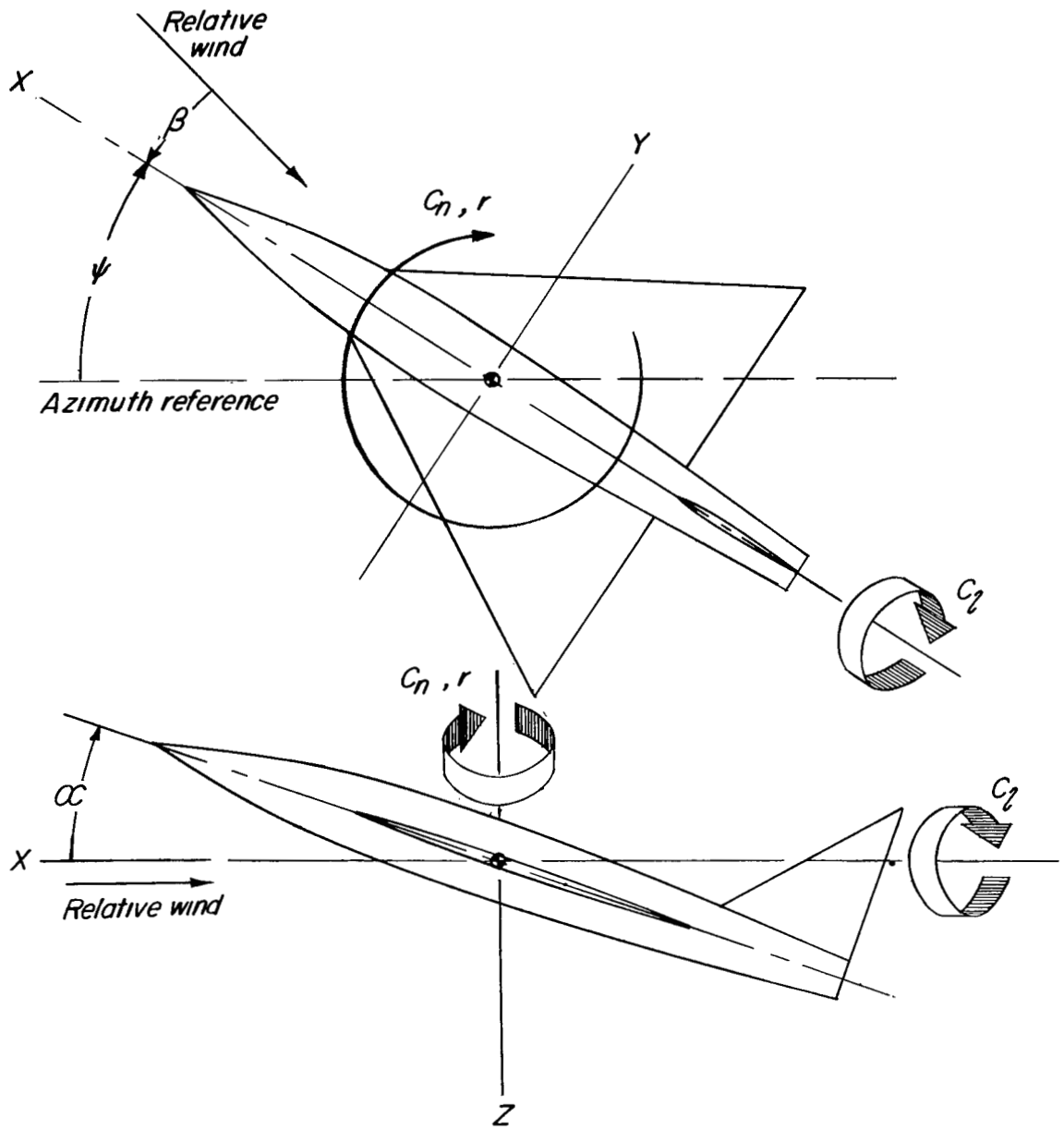

Figure 1.- Stability system of axes. (Arrows indicate positive coefficients, velocities, and displacements.)

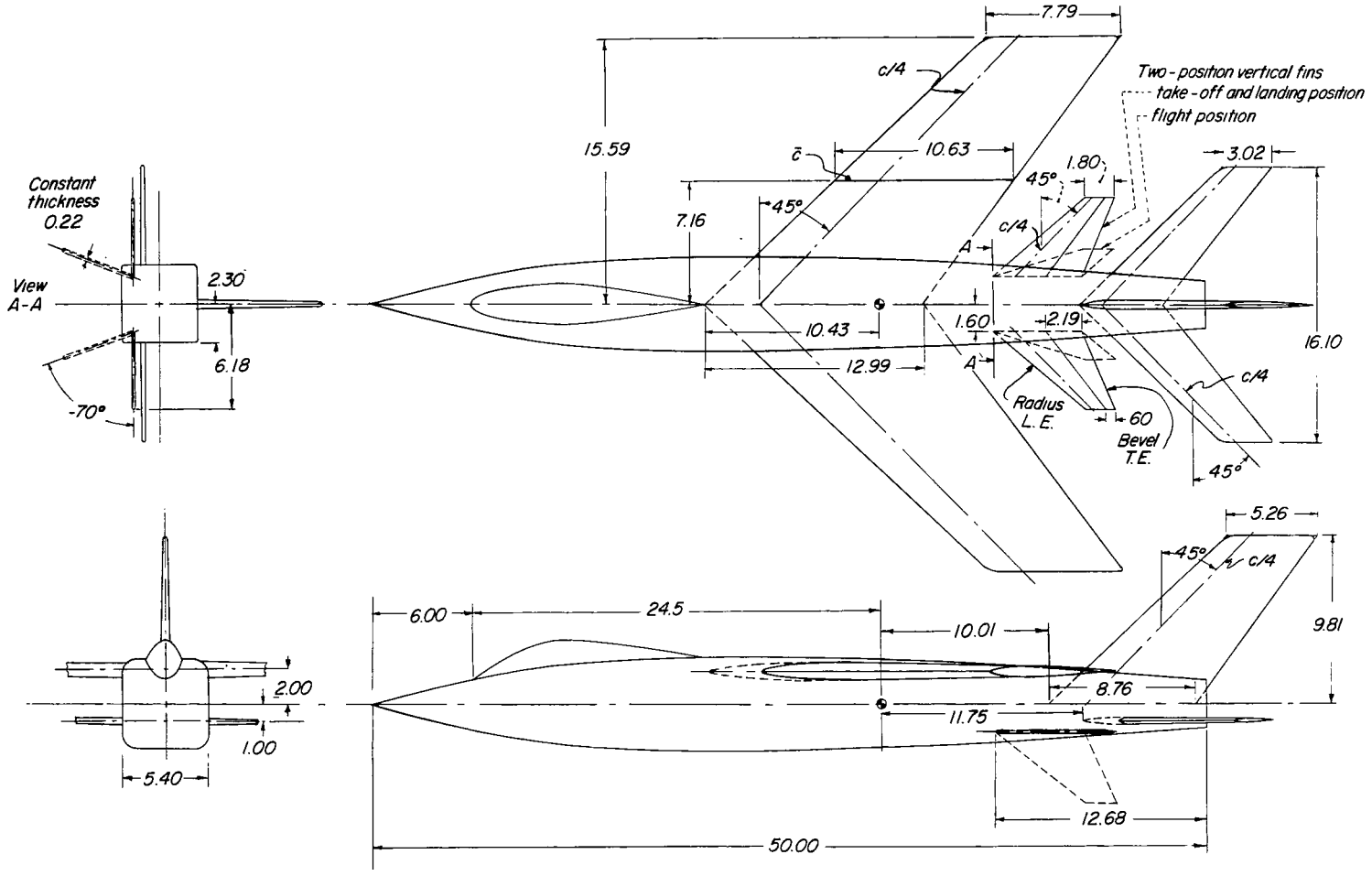

Figure 2.- Model details. (Dimensions are in inches.)

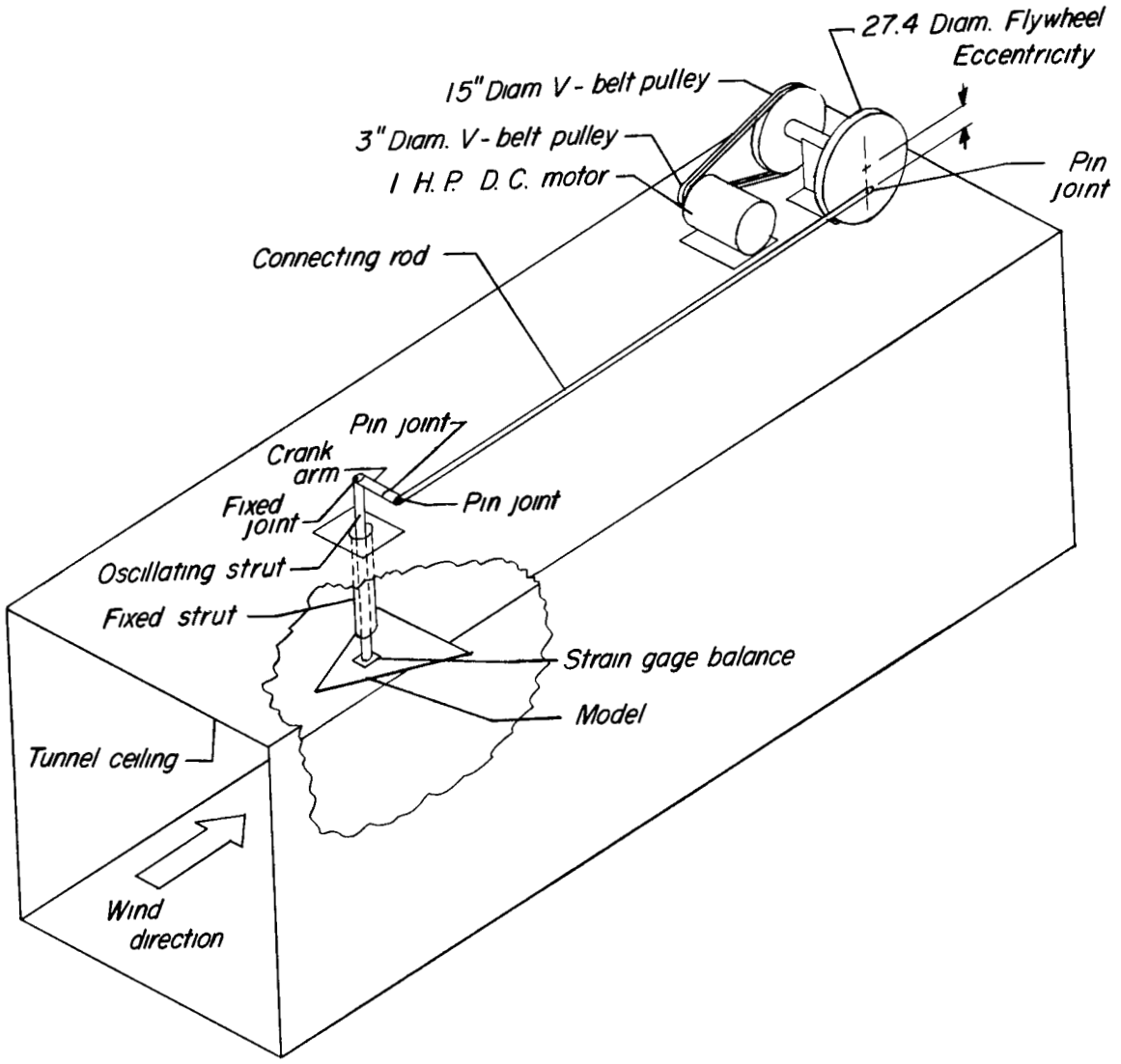

Figure 3.- Oscillation equipment.

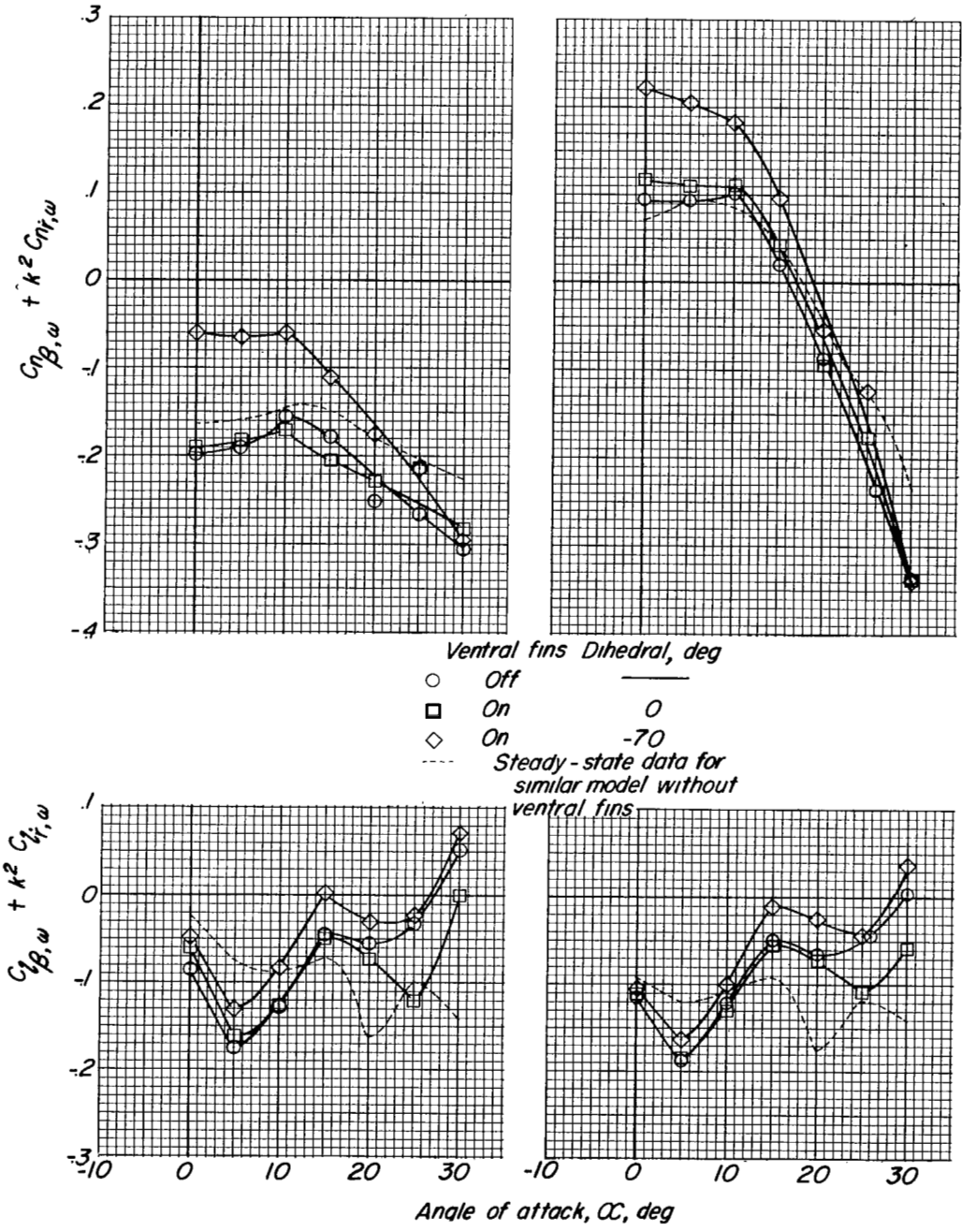

(a) Vertical and horizontal tail off.

(b) Vertical and horizontal tail on.

Figure 4.- Variation with angle of attack of the in-phase lateral oscillatory derivatives of 45° swept high-wing model.

[redacted]

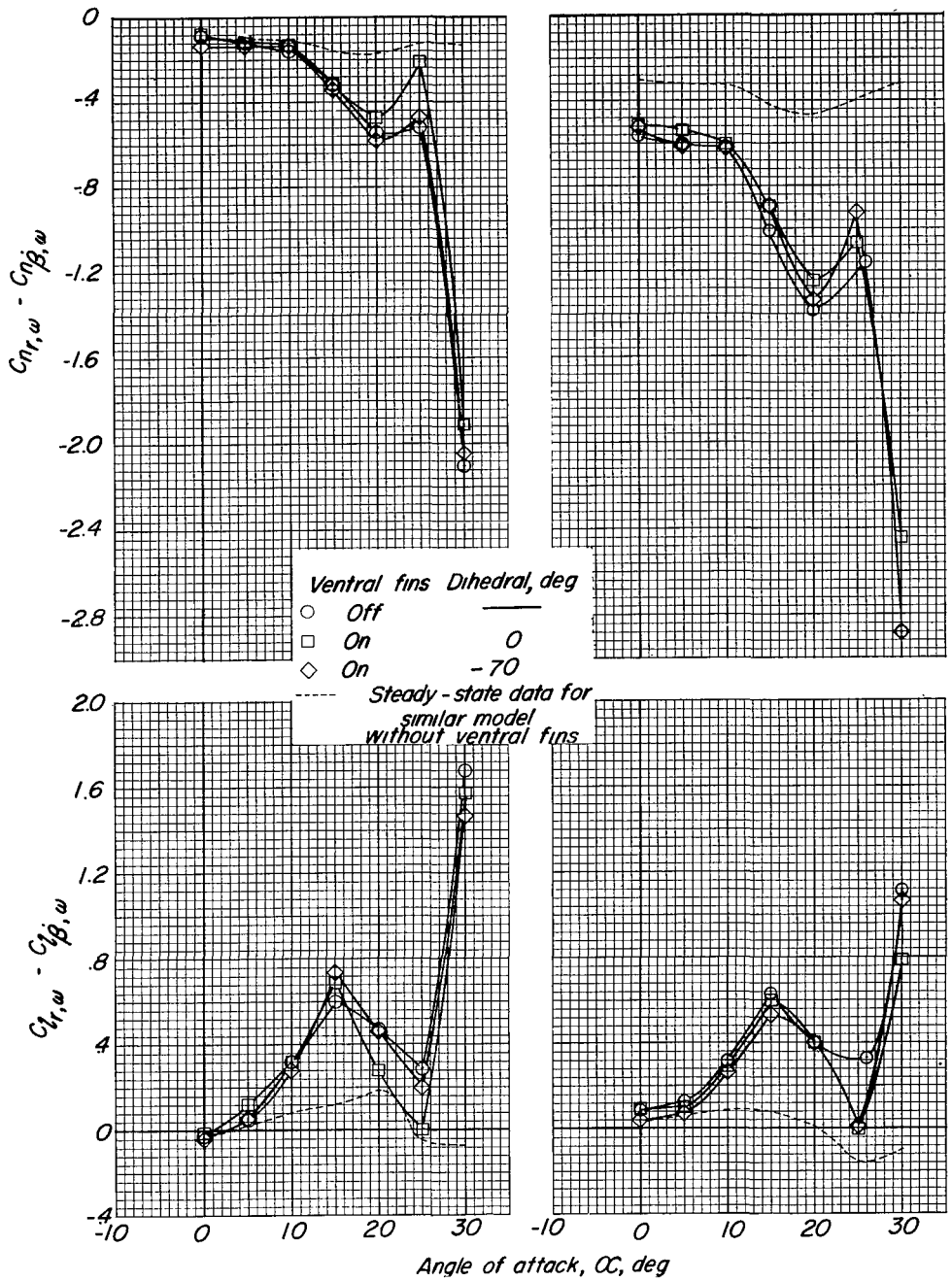

(a) Vertical and horizontal tail off.

(b) Vertical and horizontal tail on.

Figure 5.- Variation with angle of attack of the out-of-phase lateral oscillatory derivatives of 45° swept high-wing model.

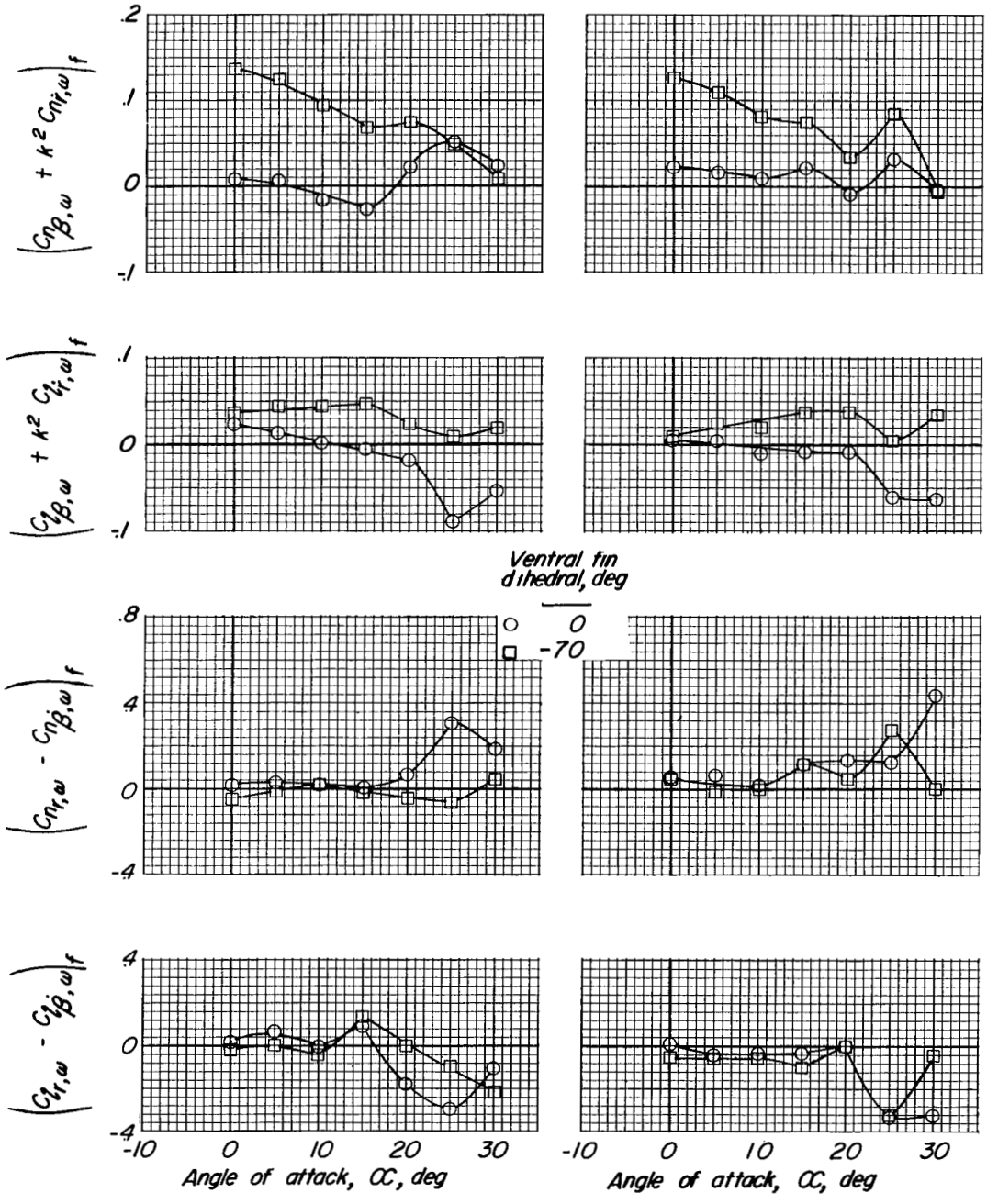

(a) Vertical and horizontal tail off.

(b) Vertical and horizontal tail on.

Figure 6.- Effect of ventral fins on lateral oscillatory derivatives of 45° swept high-wing model.